



RESEARCH PAPER

Fractional-order model of the post-disaster period: study on the earthquakes in Türkiye

Teslima Daşbaşı ^{1,‡} and Bahatdin Daşbaşı ^{2,*,‡}

¹Kayseri University, Bünyan Vocational School, Department of Property Protection and Security, 38600 Kayseri, Türkiye, ²Kayseri University, Faculty of Engineering, Architecture and Design, Department of Engineering Basic Sciences, 38280 Kayseri, Türkiye

*Corresponding Author

‡teslimadasbasi@kayseri.edu.tr (Teslima Daşbaşı); bdasbasi@kayseri.edu.tr (Bahatdin Daşbaşı)

Abstract

In this study, the mathematical model that examined the relationships between the variables of the population that continued to live in the disaster area, the population that migrated to another region, the number of newly built independent sections in the disaster area the post-disaster, and the socio-economic development index (SEDI) of the disaster area is expressed through fractional-order differential equations (FODEs) and qualitative analysis of the model is carried out. Furthermore, the relationship between migrated and non-migrated populations is presented in the model with four different functional responses. In real-world applications of the model, some earthquakes in Türkiye, which are similar to each other in many ways, are taken into account. Therefore, data after the Gölcük earthquake in 1999 are used, and parameters, derivative order, and functional response are determined by considering the minimum root mean squared error (RMSE). Then, the performance of the proposed model with these values is shown in the Elbistan earthquake in 2023. Finally, the 5-year and 10-year estimates of the non-migratory population, the migrated population, the number of newly built independent sections, and the SEDI index values are presented for Elbistan.

Keywords: Fractional-order differential equation; functional response; earthquakes; socio-economic development index; root mean squared error

AMS 2020 Classification: 26A33; 34A08; 92D25

1 Introduction

It is known that disasters have occurred in every period of history. Disasters can be defined as ecological events that suddenly change the normal life order of the society, result in loss of life and property, and create a need for external assistance depending on their size and speed of occurrence. They, which cannot be determined exactly where, when and how they will occur, have

similar following effects in terms of their consequences: economic losses and social psychological destruction, especially physical losses [1]. Disaster types, whether natural or not, are given in Table 1. There has been an increasing trend in disaster events globally from 1900 to 2022. In this context, the number of disasters averaged 56 events per year in the 1960s (reached 81 in 1966), while the average number of disasters in the last decade (2012-2022) reached 363 events per year. In addition, a total of 30748 deaths were recorded, an estimated 186 million people were negatively affected, and according to available data, these disasters caused damage worth USD 223.84 billion due to 388 disasters recorded worldwide in 2022 which are extreme heat, flood, storm, drought, forest fire, landslide, earthquake, extreme temperature and volcanic activities [2].

Table 1. Types of disasters [3]

Natural disasters		Human-Made Disasters
<i>Slow-developing natural disasters</i>	<i>Sudden Natural Disasters</i>	
-Severe cold -Drought -Famine etc.	-Earthquake -Floods -Landslides, rock falls -Avalanche -Storms, tornadoes -Volcanoes -Fires etc.	-Nuclear, biological, chemical accidents -Terrorism -Transportation accidents -Industrial accidents -Accidents caused by overcrowding -Migrants and displaced persons etc.

Today, disaster management has become an important issue due to the loss of life and large financial burden. In fact, our societies, regardless of their level of development, are still not adequately prepared for a natural or human disaster and its possible domino effects [4]. Therefore, the necessary precautions to be taken disaster-before in order to minimize the loss of life and property, as well as the necessary measures to be taken for the society to return to its normal life disaster-after, are of vital importance.

Disasters such as earthquakes and nuclear explosions or acts of terrorism in another area also occur suddenly and surprisingly. In such events, due to the effect of surprise and fear, reactions are more instinctive and individuals often tend to leave the area they are in. Migration is often considered one of the primary responses to natural disasters. Existing literature broadly recognizes the fact that disaster victims migrate from affected areas [5]. In this context, the return of individuals, who survived and migrated the post-disaster to the same region, is possible by meaning of socio-economic development of the disaster area and by building enough settlements to meet the needs. Socio-economic development involves parameters such as demography, technology, health, education, economic development, financial capacity, competitive structure and quality of life, and the data on these parameters can provide information at the regional level about what social needs are and to what extent they are met [6].

Although an earthquake is a natural event, it is inevitable that it will turn into a disaster, especially considering its duration and magnitude and the precautions taken in advance. When disasters are mentioned in Türkiye, the first thing that comes to mind is earthquakes due to its location in an earthquake zone. In this region, major earthquakes have occurred in almost every period of history, resulting in many deaths and a wave of migration. In the last 100 years, 16 earthquakes of magnitude 7 Mw and above have occurred in Türkiye, as seen Figure 1. 124558 people lost their lives in these earthquakes, and the number of buildings with moderate and more damage is about 1037108 [7]. Reverse migration after a disaster is possible with the development of the disaster area in many areas. SEDI focusing on 12 basic indicators of economic development and 12 basic indicators of social development in terms of evaluation is one of the measurable parameters

definition is considered.

In the mathematical and computer literature, scholars have mainly focused on modeling crowd dynamics and collective panic in the event of a catastrophic event [20, 21] or simulating movements to model pedestrian evacuation inside buildings [22]. Let's consider a sudden disaster that causes loss of life and property, such as an earthquake, nuclear explosion, or flood. There are few mathematical modeling studies in the literature that examine the return of individuals living in a region to their normal lives in the disaster area according to their behavior and housing needs. In addition, when looking at the studies on this subject in the literature, the number of mathematical models with ordinary differential equations (ODEs) is very low, and no mathematical model with FODEs was found.

Kumar et al. [23] examined the population in a region after a flood disaster through the ODE model, based on the classical *SIR* model, in which individuals are divided into susceptible, affected, survivor, or deceased compartments. They only presented a qualitative analysis of this model, which is widely used in different fields, without developing it.

Verdière et al. [24] modeled by ODE the temporal dynamics of human behavior during a catastrophic event. They proposed so-called PCR mathematical models that simulate sequences of individual behaviors called as Panic, Controlled, and Reflex according to the type of threat, domino effects, and the local environment. In their model, the population that continues its normal daily life is denoted by Q , individuals with uncontrolled behavior are denoted by r and p , and individuals with controlled behavior are denoted by c . At the beginning, the total population N is in Q_1 , subpopulation of Q . A post-disaster occurs, all individuals move to compartment r at a certain rate, individuals in r , those showing panic behavior at certain rates, move to compartment p , and those showing controlled behavior move to compartment c . Finally, at a certain rate, there is a transition from c to the Q_2 compartment in which individuals continue their daily life. Furthermore, the authors assumed reciprocal transition between r , c , and p compartments. They numerically illustrated their model for the earthquake in Haiti and Japan in 2010.

In our proposed model, the interaction between the population that migrated and those that did not migrate post-disaster was expressed with different functional responses, and then the functional response closest to the real data was determined. Therefore, the reason for using four responses, which are frequently mentioned in the literature, is to increase the performance of the model by determining the response that gives the minimum RMSE value. In fact, four different mathematical models are presented as a single model in the manuscript.

Earthquakes, landslides, floods, volcanic eruptions, hurricanes, and tornadoes, which have been repeated countless times since the world was formed 4.6 billion years ago, are actually ordinary events that give our planet its current appearance. Therefore, disasters are intertwined with humanity and are inevitable. Many researchers around the world have carried out many studies on the effects of disasters. However, there are very few studies in the literature on post-disaster migration mobility and changes in population projection, which aim to determine in advance the size of the workforce that will be needed in the future and to prepare the infrastructure and opportunities accordingly.

In this study, the scenario immediately after a disaster, such as an earthquake or flood, that causes a sudden loss of life and property is discussed. All individuals living in the region naturally exhibit reflexive behavior. Some of them migrate to another region due to a lack of shelter or panic behavior, and their population size is shown as M in the model. The rest of them continue to live in the disaster area by exhibiting controlled behavior, and their population size in the model is denoted by S . The number of new buildings built to replace independent sections that were demolished or decided to be demolished after the disaster is also indicated by R . Moreover, the SEDI of the region is presented with I . In this sense, the relationship among the dimensions of the

variables S , M , R , and I has been modeled mathematically through FODEs in the Caputo meaning. In this way, due to the definition of fractional derivative, the natural delay in the relevant disaster scenario was also taken into account.

Therefore, the differences in the presented study from the literature can be listed as follows:

- FODEs are used in the model.
- The different functional responses are used in the model.
- According to the real values, the parameter values and the derivative-order with minimum RMSE have been obtained.
- Predictions are made for future population projection, SEDI, and independent section numbers.

The remainder of the study is organized as follows.

- Some basic definitions and theorems used in the definition and analysis of the model are given in [Section 2](#).
- The proposed mathematical model is formulated in [Section 3](#). It was also presented respectively in:
 - The positivity, boundedness, and non-negative of solutions of the model,
 - Different possible equilibrium points of the model and,
 - Stability analysis of the equilibrium points.
- The estimation of the parameters of the proposed model is given in [Section 4](#). Therefore, the data set was created, parameters with minimum RMSE were obtained, the fractional order was determined to obtain lower RMSE, and numerically simulated results for Elbistan of our proposed model have been presented.
- Finally, in [Section 5](#), we have presented some of the main outcomes of the present work.

2 Preliminaries and definitions

In this section, we have discussed some functional answers for the Lotka-Volterra system. Later, we present some useful definitions and properties of fractional derivatives. In addition, some properties regarding the existence and signs of the roots of the polynomials used in the study are given.

Definition 1 *The Lotka-Volterra predator-prey model consists of two differential equations, the first equation for the prey and the second equation for the predator, and is as follows:*

$$\frac{dx}{dt} = ax - \gamma xy \quad \text{and} \quad \frac{dy}{dt} = -cy + exy,$$

where $a, \gamma, c, e > 0$. The terms $\gamma xy = F(x, y)$ and $exy = G(x, y)$ in this system are called functional and numerical responses, respectively [25].

Some functional responses are Holling Type I for $F(x, y) = \gamma xy$, $\gamma > 0$, Holling Type II for $F(x, y) = \frac{\gamma xy}{x+b}$, $\gamma, b > 0$, Holling Type III for $F(x, y) = \frac{\gamma x^2 y}{x^2+b}$, $\gamma, b > 0$ and Ivlev for $F(x, y) = \gamma y (1 - e^{-bx})$, $\gamma, b > 0$ [26, 27].

In this study, the above-mentioned functional responses were used for the relationship between post-disaster migratory and non-migratory populations. The functional responses used in the manuscript can be briefly explained as follows. Let us consider two species that have certain sizes at reference time t and, moreover, interact with each other. Functions describing their varying population sizes are modeled in a continuous framework. Changes depending on the relationship between these functions can be explained by functional response. Functional response [28] is one

of the oldest and most common mathematical constructs used to describe and make prospective predictions about the nutritional interaction between a consumer and a resource. This response describes the feeding rate of a consumer based on its density in its environment. The most common of these are Holling type I-III responses [27] and Ivlev response [29].

Type I functional response supposes a linear increase in intake rate with food density, either for all food densities or only for maximum food densities, beyond which the intake rate is constant. Linear increase reckons for the following: the time a consumer needs to process a food item is neglectable or that consuming food does not prevent foraging.

Type II functional response is qualified by a slowing rate of intake, following from the presumption that the consumer is restricted by his or her food processing capacity. Also, the functional response is commonly modeled through a rectangular hyperbola.

Type III functional response is alike to type II in that at high levels of prey density, saturation occurs. At low prey density levels, the graphical connection of the number of prey consumed and the density of the prey population is a super linearly increasing function of prey consumed by predators.

In Ivlev's functional response, the maximal rate of predation and decline in hunting drive are represented by the positive constant γ and b , respectively [30].

Definition 2 (Caputo Fractional Derivative) [31] $0 < \phi \leq 1$ for the function $u: C^n[0, \infty] \rightarrow \mathbb{R}$ is defined as

$${}^C D_t^\phi(u(t)) = \frac{1}{\Gamma(n-\phi)} \int_0^t \frac{1}{(t-z)^{\phi+1-n}} \frac{d^n}{dz^n} u(z) dz, \quad (1)$$

where $C^n[0, \infty]$ is a n times continuously differentiable function and Gamma function is defined by $\Gamma(\cdot)$ such that $n - 1 < \phi < n$.

Lemma 1 [32] Let $0 < \phi \leq 1$. Suppose that $u(t) \in C[a, b]$ and ${}^C D_{t_0}^\phi u(t) \in C[a, b]$.

- If ${}^C D_{t_0}^\phi u(t) \geq 0, \forall t \in (a, b)$, then $u(t)$ is a non-decreasing function.
- If ${}^C D_{t_0}^\phi u(t) \leq 0, \forall t \in (a, b)$, then $u(t)$ is a non-increasing function.

Theorem 1 [33, 34] Consider the following fractional-order system:

$$\begin{aligned} {}^C D_t^\phi(u(t)) &= f(t, u(t)), \\ u(t_0) &= u_0, \end{aligned} \quad (2)$$

where ${}^C D_t^\phi$ is Caputo's derivative of the order $0 < \phi \leq 1$ and $f(t, u(t)) : \mathbb{R}^+ \times \mathbb{R}^n \rightarrow \mathbb{R}^n$ is a vector field. The equilibrium points of this system are locally asymptotically stable (LAS) if all eigenvalues λ_i of the Jacobian matrix $\frac{\partial f(t, u)}{\partial u}$ evaluated at the equilibrium points satisfy the following condition:

$$|\arg \lambda_i| > \frac{\phi \pi}{2}. \quad (3)$$

Let's consider system (2) for $u = (u_1 \ u_2)^T$. In this case, the characteristic equation is

$$p(\lambda) = \lambda^2 + a_1 \lambda + a_2 = 0. \quad (4)$$

The conditions for LAS of the equilibrium point are either Routh–Hurwitz conditions given as

$$a_1, a_2 > 0, \tag{5}$$

or:

$$a_1 < 0, 4a_2 > (a_1)^2, \left| \tan^{-1} \left(\frac{\sqrt{4a_2 - (a_1)^2}}{a_1} \right) \right| > \frac{\alpha\pi}{2}, \tag{6}$$

[35].

Theorem 2 (Descartes’s Rule of Signs) [36] "Let

$$p(x) = a_0x^{b_0} + a_1x^{b_1} + \dots + a_nx^{b_n}, \tag{7}$$

denote a polynomial with nonzero real coefficient a_i , where b_i are integers satisfying $0 \leq b_0 < b_1 < b_2 < \dots < b_n$. Then the number of positive real zeros of $p(x)$ (counted with multiplicities) is either equal to the number of variations in sign in the sequence a_0, a_1, \dots, a_n of the coefficients or less than that by an even whole number. The number of negative zeros of $p(x)$ (counted with multiplicities) is either equal to the number of variations in sign in the sequence of the coefficients of $p(-x)$ or less than that by an even whole number."

3 Methodology

Fractional-order model

Let t denote the time parameter and the independent variable. The dependent variables whose changes are being examined post-disaster in the proposed model consisting of FODEs in the Caputo meaning are given in Table 2. In addition, the parameters used in the model and whose

Table 2. State variables in the proposed mathematical model

Variable	Definition	Explanation
$S(t)$	The population number at time t who continues to live the post-disaster in the region where they lived before the disaster	These are people who, the post-disaster, continue to live in their pre-disaster residence or a temporary place in the same area
$M(t)$	The population number at time t migrating to another region the post-disaster	These are people settled another region by leaving the area they were in before the disaster, temporarily or permanently, the post-disaster
$R(t)$	The number at time t of newly built independent sections	These are the number of newly built independent sections to replace buildings that were demolished or decided to be demolished post-disaster
$I(t)$	The SEDI at time t	Socio-Economic Performance Index, which is a measurable indicator of the development of the disaster area

approximate values will be estimated later in numerical studies by using the actual values of the variables are given in Table 3.

Table 3. Parameters used in the mathematical model and their meanings

Parameter	Definition
θ_S	Constant increase rate of the population living in the region where they lived before the disaster,
η	The return rate to the disaster area with respect to SEDI with controlled behavior of individuals who migrated with panic behavior,
μ	The return rate of individuals to the region where they were before the disaster, thanks to the newly built independent sections,
$f_i(M)$	Functions for $i = 1, 2, 3, 4$, which represent the functional and numerical responses, are Holling Type 1-3 and Ivlev functions, respectively,
γ	As a result of the contact between migrated and non-migrated populations, the rate of return of the migrated population to the region where they were before the disaster,
ε	Migration rate to the region the post-disaster according to the SEDI,
v_S	Natural mortality rate of the population living in the destruction zone the post-disaster,
θ_M	Constant increase rate of the migrated population,
v_M	Natural mortality rate of the migrated population the post-disaster,
r_R	The increase rate of newly built independent sections,
C_R	Carrying capacity of the newly built independent section,
σ	The rate of independent sections built in proportion to SEDI,
β	Decrease rate of newly built independent sections,
θ	Constant rate of SEDI,
ω	Decrease rate of SEDI.

Thus, the proposed fractional-order model in the Caputo meaning is

$$\begin{aligned}
 {}^C D_{t_0}^\phi S &= \theta_S + \eta MI + \mu MR + \gamma S f_i(M) + \varepsilon I - v_S S, \\
 {}^C D_{t_0}^\phi M &= \theta_M - \eta MI - \mu MR - \gamma S f_i(M) - v_M M, \\
 {}^C D_{t_0}^\phi R &= r_R R \left(1 - \frac{R}{C_R}\right) + \sigma RI - \beta R, \\
 {}^C D_{t_0}^\phi I &= \theta_I - \omega I, \\
 S &\equiv S(t), M \equiv M(t), R \equiv R(t), I \equiv I(t), \\
 S(t_0) &= S_0, R(t_0) = R_0, M(t_0) = M_0, I(t_0) = I_0 \text{ such that } S_0, R_0, M_0, I_0 > 0,
 \end{aligned}
 \tag{8}$$

where $t \geq t_0 \geq 0$, $\phi \in (.0, 1|$. and ${}^C D_{t_0}^\phi$ denotes the Caputo operator. The parameters in system (8) satisfy

$$\theta_S, \eta, \mu, \gamma, \varepsilon, v_S, \theta_M, v_M, r_R, C_R, \sigma, \beta, \theta, \omega > 0.
 \tag{9}$$

Additionally, mathematical expressions of the functions $f_i(M)$ for $i = 1, 2, 3, 4$ are shown in [Table 4](#).

Table 4. Functional responses used in Eqs. (8) for $b > 0$

Response Type	Function ($f_i(M)$)
Holling Type-1	$f_1(M) = M$
Holling Type-2	$f_2(M) = \frac{M}{M+b}$
Holling Type-3	$f_3(M) = \frac{M^2}{M^2+b}$
Ivlev Type	$f_4(M) = 1 - e^{-bM}$

Theorem 3 *There is one solution of the equation in (8) with non-negative initial conditions.*

Proof Existence and uniqueness of system (8) will be displayed in the map $\Omega \times (0; T]$ where

$$\Omega = \{(S, M, R, I) \in \mathbb{R}_+^4 : \max(|S|, |M|, |R|, |I|) \leq \zeta\}. \tag{10}$$

Reference [37] is taken into account for the proof. We express $X = (S, M, R, I)$ and $\bar{X} = (\bar{S}, \bar{M}, \bar{R}, \bar{I})$. Consider a mapping

$$G(X) = (G_1(X), G_2(X), G_3(X), G_4(X)), \tag{11}$$

and

$$\begin{aligned} G_1(X) &= \theta_S + \eta MI + \mu MR + \gamma S f_i(M) + \varepsilon I - v_S S, \\ G_2(X) &= \theta_M - \eta MI - \mu MR - \gamma S f_i(M) - v_M M, \\ G_3(X) &= r_R R (1 - \frac{R}{C_R}) + \sigma RI - \beta R, \\ G_4(X) &= \theta - \omega I. \end{aligned} \tag{12}$$

First, consider the functions in (12). For any X, \bar{X} , one can find the followings by:

$$\begin{aligned} \|G(X) - G(\bar{X})\| &= |(\theta_S + \eta MI + \mu MR + \gamma S f_i(M) + \varepsilon I - v_S S) - (\theta_S + \eta \bar{M}\bar{I} + \mu \bar{M}\bar{R} + \gamma \bar{S} f_i(\bar{M}) + \varepsilon \bar{I} - v_S \bar{S})| \\ &+ |(\theta_M - \eta MI - \mu MR - \gamma S f_i(M) - v_M M) - (\theta_M - \eta \bar{M}\bar{I} - \mu \bar{M}\bar{R} - \gamma \bar{S} f_i(\bar{M}) - v_M \bar{M})| \\ &+ |(r_R R (1 - \frac{R}{C_R}) + \sigma RI - \beta R) - (r_R \bar{R} (1 - \frac{\bar{R}}{C_R}) + \sigma \bar{R}\bar{I} - \beta \bar{R})| + |(\theta - \omega I) - (\theta - \omega \bar{I})|, \end{aligned}$$

$$\begin{aligned} \|G(X) - G(\bar{X})\| &= |\eta MI - \eta \overbrace{(M\bar{I} - M\bar{I})}^{=0} - \eta \bar{M}\bar{I} + \mu MR - \mu \overbrace{(M\bar{R} - M\bar{R})}^{=0} - \mu \bar{M}\bar{R} + \gamma S f_i(M) - \\ &\gamma \overbrace{(S\bar{f}_i(M) - S\bar{f}_i(M))}^{=0} - \gamma \bar{S} f_i(\bar{M}) + \varepsilon I - \varepsilon \bar{I} - v_S S + v_S \bar{S}| + |-\eta MI - \eta \overbrace{(M\bar{I} - M\bar{I})}^{=0} + \eta \bar{M}\bar{I} - \mu MR - \\ &\mu \overbrace{(R\bar{M} - \bar{R}M)}^{=0} + \mu \bar{M}\bar{R} - \gamma S f_i(M) - \gamma \overbrace{(S\bar{f}_i(M) - S\bar{f}_i(M))}^{=0} + \gamma \bar{S} f_i(\bar{M}) - v_M M + v_M \bar{M}| + |r_R R - r_R \bar{R} - \\ &\frac{r_R}{C_R} R^2 + \frac{r_R}{C_R} \bar{R}^2 + \sigma RI - \sigma \overbrace{(R\bar{I} - R\bar{I})}^{=0} - \sigma \bar{R}\bar{I} - \beta R + \beta \bar{R}| + |-\omega(I - \bar{I})|, \end{aligned}$$

$$\begin{aligned} \|G(X) - G(\bar{X})\| &= |+\eta M(I - \bar{I}) + \eta \bar{I}(M - \bar{M}) + \mu M(R - \bar{R}) + \mu \bar{R}(M - \bar{M}) + \gamma f_i(M)(S - \bar{S}) + \\ &\gamma \bar{S}(f_i(M) - f_i(\bar{M})) + \varepsilon(I - \bar{I}) - v_S(S - \bar{S})| + |-\eta M(I - \bar{I}) - \eta \bar{I}(M - \bar{M}) - \mu M(R - \bar{R}) - \mu \bar{R}(M - \\ &\bar{M}) - \gamma f_i(M)(S - \bar{S}) - \gamma \bar{S}(f_i(M) - f_i(\bar{M})) - v_M(M - \bar{M})| + |r_R(R - \bar{R}) - \frac{r_R}{C_R}(R - \bar{R})(R + \bar{R}) + \\ &\sigma R(I - \bar{I}) - \sigma \bar{I}(R - \bar{R}) - \beta(R - \bar{R})| + \omega|I - \bar{I}|, \end{aligned}$$

and

$$\begin{aligned} \|G(X) - G(\bar{X})\| &\leq (v_S + 2\gamma f_i(M))|S - \bar{S}| + (2\mu \bar{R} + 2\eta \bar{I} + v_M)|M - \bar{M}| \\ &+ (2\mu M + r_R + \beta + \sigma \bar{I} + \frac{r_R}{C_R}(R + \bar{R}))|R - \bar{R}| \\ &+ (2\eta M + \varepsilon + \sigma R + \omega)|I - \bar{I}| + 2\gamma \bar{S} \overbrace{|f_i(M) - f_i(\bar{M})|}^*. \end{aligned} \tag{13}$$

If the expression marked * in Ineq. (13) is taken into account throughout Table 4, then we have

$$|f_i(M) - f_i(\bar{M})| = \left\{ \begin{array}{l} |M - \bar{M}| \text{ for } i = 1, \\ \frac{b|M - \bar{M}|}{(M+b)(\bar{M}+b)} \leq \frac{|M - \bar{M}|}{b} \text{ for } i = 2, \\ \frac{b(M+\bar{M})|M - \bar{M}|}{(M^2+b)(\bar{M}^2+b)} \leq \frac{2\zeta|M - \bar{M}|}{b} \text{ for } i = 3, \\ \left. \begin{array}{l} \text{by Taylor Expansion} \\ |b(\bar{M} - M) + \frac{b^2(\bar{M}^2 - M^2)}{2!} + \dots + \frac{b^n(\bar{M}^n - M^n)}{n!}| \\ |M - \bar{M}| \left| b + \frac{b^2(\bar{M}+M)}{2!} + \dots + \frac{b^n(\sum_{j=1}^n \bar{M}^{n-j} M^{j-1})}{n!} \right| \\ \leq |M - \bar{M}| \left(b + \frac{\zeta b^2}{1!} + \frac{\zeta^2 b^3}{2!} + \dots + \frac{\zeta^{n-1} b^n}{(n-1)!} \right) \end{array} \right\} \text{ for } i = 4, \end{array} \right\},$$

and so,

$$|f_i(M) - f_i(\bar{M})| \leq \zeta_M |M - \bar{M}|, \tag{14}$$

where

$$\zeta_M = \max \left\{ 1, \frac{1}{b}, \frac{2\zeta}{b}, \left(b + \frac{\zeta b^2}{1!} + \frac{\zeta^2 b^3}{2!} + \dots + \frac{\zeta^{n-1} b^n}{(n-1)!} \right) \right\}.$$

In this case, Ineq. (14) is obtained as follows:

$$\|G(X) - G(\bar{X})\| \leq \varphi_1 |S - \bar{S}| + \varphi_2 |M - \bar{M}| + \varphi_3 |R - \bar{R}| + \varphi_4 |I - \bar{I}|,$$

where

$$\begin{aligned} \varphi_1 &= (v_S + 2\gamma f_i(\zeta)\zeta_S), \\ \varphi_2 &= (2\mu\zeta + 2\eta\zeta + v_M + 2\gamma(\zeta)\zeta_M), \\ \varphi_3 &= (2\mu\zeta + r_R + \beta + \sigma\zeta + 2\frac{r_R}{C_R}\zeta), \\ \varphi_4 &= (2\eta\zeta + \varepsilon + \sigma\zeta + \omega). \end{aligned} \tag{15}$$

Consequently, it is acquired $\|G(X) - G(\bar{X})\| \leq L\|X - \bar{X}\|$ where $L = \max(\varphi_1, \varphi_2, \varphi_3, \varphi_4)$, and so, $G(X)$ met the Lipschitz condition. In summary, the existence and uniqueness of solutions of (8) is demonstrated.

Theorem 4 *The FOS's solutions in (8), starting in \mathbb{R}_+^4 are uniformly bounded.*

Proof The approach used in [38] was considered.

i. Consider the fourth equation in (8). Therefore, we have ${}^C D_t^\phi I + \omega I = \theta_I$. Considering the standard comparison theorem for fractional-order, it is obtained as follows:

$$I(t) = \left(I(0) - \frac{\theta_I}{\omega} \right) E_{\phi,1}(-\omega t^\phi) + \frac{\theta_I}{\omega},$$

and so,

$$\lim_{t \rightarrow \infty} I(t) = \frac{\theta_I}{\omega}, \tag{16}$$

where E_α is the Mittag–Leffler function.

ii. From the third equation in (8), we have the followings:

$${}^C D_t^\phi R + \beta R = \frac{r_R}{C_R} \left(\frac{(r_R + \sigma I)}{2 \frac{r_R}{C_R}} \right)^2 - \frac{r_R}{C_R} \left(R - \left(\frac{(r_R + \sigma I)}{2 \frac{r_R}{C_R}} \right) \right)^2 \leq \frac{r_R}{C_R} \left(\frac{(r_R + \sigma I)}{2 \frac{r_R}{C_R}} \right)^2,$$

$$R(t) \leq \left(R(0) - \frac{1}{\beta} \frac{r_R}{C_R} \left(\frac{(r_R + \sigma I)}{2 \frac{r_R}{C_R}} \right)^2 \right) E_{\phi,1}(-\beta t^\phi) + \frac{1}{\beta} \frac{r_R}{C_R} \left(\frac{(r_R + \sigma I)}{2 \frac{r_R}{C_R}} \right)^2,$$

and

$$\lim_{t \rightarrow \infty} R(t) = \frac{1}{\beta} \frac{r_R}{C_R} \left(\frac{(r_R + \sigma \frac{\theta_I}{\omega})}{2 \frac{r_R}{C_R}} \right)^2. \tag{17}$$

iii. Now let’s consider the first and second equations of the system (8) for $N(t) = S(t) + M(t)$. In this case, we have the following:

$${}^C D_t^\phi S(t) + {}^C D_t^\phi M(t) = {}^C D_t^\phi N(t) = \theta_S + \theta_M + \varepsilon I - v_S S - v_M M,$$

$${}^C D_t^\phi N(t) + v_S S + v_M M = (\theta_S + \theta_M + \varepsilon I),$$

and

$${}^C D_t^\phi N(t) + v_N N \leq (\theta_S + \theta_M + \varepsilon I),$$

where $\min\{v_S, v_M\} = v_N$. Therefore, it is found that

$$N(t) \leq \left(N(0) - \frac{\theta_S + \theta_M + \varepsilon I}{v_N} \right) E_{\phi,1}(-v_N t^\phi) + \frac{\theta_S + \theta_M + \varepsilon I}{v_N},$$

and

$$\lim_{t \rightarrow \infty} N(t) = \frac{\theta_S + \theta_M + \varepsilon \frac{\theta_I}{\omega}}{v_N}. \tag{18}$$

As a result, the solutions starting in \mathbb{R}_+^4 of system (8) are uniformly bounded to the region Ω , in which $\Omega := \{(S, M, R, I) \in \mathbb{R}_+^4 : S + M \leq \frac{\theta_S + \theta_M + \varepsilon \frac{\theta_I}{\omega}}{v_N} + \varepsilon_1, R(t) \leq \frac{1}{\beta} \frac{r_R}{C_R} \left(\frac{(r_R + \sigma \frac{\theta_I}{\omega})}{2 \frac{r_R}{C_R}} \right)^2 + \varepsilon_2, I(t) \leq \frac{\theta_I}{\omega} + \varepsilon_3, \varepsilon_1, \varepsilon_2, \varepsilon_3 > 0\}$.

Theorem 5 *The FOS’s solutions in (8) starting in \mathbb{R}_+^4 are non-negative.*

Proof For proof, the approach used in [38] was taken into account. From the first and second equations of Eqs. (8), it has been assumed that $N(t) = S(t) + M(t)$ where $N(t) \rightarrow 0$ means $S(t) \rightarrow 0$ and $M(t) \rightarrow 0$. Therefore, the followings ${}^C D_t^\phi I(t)|_{I=0} = \theta_I > 0, {}^C D_t^\phi N(t)|_{N=0} =$

$\theta_S + \theta_M + \varepsilon I > 0$, ${}^C D_t^\phi R(t)|_{R=0} = 0$ are found. In this sense, the solutions are non-negative.

Equilibrium points of proposed model

$E(\bar{S}, \bar{M}, \bar{R}, \bar{I})$ points found by solving the equation system ${}^C D_t^\phi S(t) = 0, {}^C D_t^\phi M(t) = 0, {}^C D_t^\phi R(t) = 0, {}^C D_t^\phi I(t) = 0$ obtained from the system (8) are the equilibrium points. In this case,

$$\begin{aligned} \theta_S + \eta \bar{M} \bar{I} + \mu \bar{M} \bar{R} + \gamma \bar{S} f_i(\bar{M}) + \varepsilon \bar{I} - v_S \bar{S} &= 0, & (a) \\ \theta_M - \eta \bar{M} \bar{I} - \mu \bar{M} \bar{R} - \gamma \bar{S} f_i(\bar{M}) - v_M \bar{M} &= 0, & (b) \\ r_R \bar{R} (1 - \frac{\bar{R}}{C_R}) + \sigma \bar{R} \bar{I} - \beta \bar{R} &= 0, & (c) \\ \theta_I - \omega \bar{I} &= 0, & (d) \end{aligned} \tag{19}$$

is obtained. From Eqs. (19), it is found as

$$\begin{aligned} \bar{S} &= \frac{(\theta_S + \theta_M + \varepsilon \bar{I} - v_M \bar{M})}{v_S} \text{ when } \bar{I} > \frac{v_M \bar{M} - (\theta_S + \theta_M)}{\varepsilon}, & (a) \\ \bar{R}_1 &= 0 \text{ or } \bar{R}_2 = \frac{r_R + \sigma \bar{I} - \beta}{\frac{r_R}{C_R}} \text{ when } \bar{I} > \frac{\beta - r_R}{\sigma}, & (b) \\ \bar{I} &= \frac{\theta_I}{\omega}. & (c) \end{aligned} \tag{20}$$

In addition, the equations for \bar{M} from Eq. (19) -(b) according to each function in Table 4 are as follows:

$$\begin{aligned} \bar{M} &= \frac{\theta_M}{(\gamma \bar{S} + (\eta \bar{I} + \mu \bar{R} + v_M))}, & \text{for } i = 1, & (a) \\ \bar{M}^2 + [b + \frac{(\gamma \bar{S} - \theta_M)}{(\eta \bar{I} + \mu \bar{R} + v_M)}] \bar{M} - \frac{b \theta_M}{(\eta \bar{I} + \mu \bar{R} + v_M)} &= 0, & \text{for } i = 2, & (b) \\ \bar{M}^3 + \frac{(\gamma \bar{S} - \theta_M)}{(\eta \bar{I} + \mu \bar{R} + v_M)} \bar{M}^2 + b \bar{M} - \frac{b \theta_M}{(\eta \bar{I} + \mu \bar{R} + v_M)} &= 0, & \text{for } i = 3, & (c) \\ (1 - e^{-bM}) \frac{\gamma \bar{S}}{(\eta \bar{I} + \mu \bar{R} + v_M)} &= (\frac{\theta_M}{(\eta \bar{I} + \mu \bar{R} + v_M)} - \bar{M}), & \text{for } i = 4, & (d) \end{aligned} \tag{21}$$

where \bar{S}, \bar{R} and \bar{I} are shown in Eqs. (20). Let us consider Ineqs. in (20). If at least one value \bar{M} can be obtained from the Eqs. (21), when

$$\frac{v_M \bar{M} - (\theta_S + \theta_M)}{\varepsilon} < \bar{I}, \tag{22}$$

for \bar{R}_1 , and when

$$\max\{\frac{\beta - r_R}{\sigma}, \frac{v_M \bar{M} - (\theta_S + \theta_M)}{\varepsilon}\} < \bar{I}, \tag{23}$$

for \bar{R}_2 . Therefore, the existence of an equilibrium point can be said. In this case, let us show the existence of the component \bar{M} of the equilibrium point from the Eqs. (21).

- i. Consider the Eq. (21)-(a). It is clear that $\bar{M} > 0$ due to Ineqs. (9), (22) and (23). Thus, the equilibrium points $E_1^{(1)}(\bar{S}, \bar{M}, \bar{R}_1, \bar{I})$ or $E_1^{(1)}(\bar{S}, \bar{M}, \bar{R}_2, \bar{I})$ are obtained.
- ii. Now let us consider equation (21)-(b). In this case, the equation for \bar{M} is

$$\bar{M}^2 + \zeta_1 \bar{M} + \zeta_2 = 0, \tag{24}$$

where

$$\zeta_1 = \left(b + \frac{(\gamma\bar{S}-\theta_M)}{(\eta\bar{I}+\mu\bar{R}+v_M)} \right), \text{ and } \zeta_2 = -\frac{b\theta_M}{(\eta\bar{I}+\mu\bar{R}+v_M)}. \tag{25}$$

From the Ineqs. (9), (22) and (23), it can be seen that $\zeta_2 < 0$. This shows that Eq. (24) has one positive \bar{M} value. In this case, there is the equilibrium points $E_2^{(1)}(\bar{S}, \bar{M}, \bar{R}_1, \bar{I})$ or $E_2^{(1)}(\bar{S}, \bar{M}, \bar{R}_2, \bar{I})$.

iii. Considering (21)-(c), the equation for \bar{M} is the following:

$$\bar{M}^3 + \vartheta_1\bar{M}^2 + \vartheta_2\bar{M} + \vartheta_3 = 0, \tag{26}$$

where $\vartheta_1 = \frac{(\gamma\bar{S}-\theta_M)}{(\eta\bar{I}+\mu\bar{R}+v_M)}$, $\vartheta_2 = b$, $\vartheta_3 = -\frac{b\theta_M}{(\eta\bar{I}+\mu\bar{R}+v_M)}$. Due to the Ineqs. (9), (22) and (23), it is obvious that $\vartheta_2 > 0$, $\vartheta_3 < 0$. According to Descartes' rule of signs in Theorem 2, one can reach the following conclusions for the \bar{M} roots of Eq. (26):

- If $\vartheta_1 \geq 0$,

$$\bar{I} \geq \frac{v_M\bar{M} + \frac{\theta_M}{\gamma}v_S - (\theta_S + \theta_M)}{\varepsilon}, \tag{27}$$

then Eq. (26) has one positive root, denoted by $E_3^{(1)}(\bar{S}, \bar{M}, \bar{R}_1, \bar{I})$ or $E_3^{(1)}(\bar{S}, \bar{M}, \bar{R}_2, \bar{I})$.

- If $\vartheta_1 < 0$,

$$\bar{I} < \frac{v_M\bar{M} + \frac{\theta_M}{\gamma}v_S - (\theta_S + \theta_M)}{\varepsilon}, \tag{28}$$

then Eq. (26) has one or three positive roots denoted by $E_3^{(i)}(\bar{S}, \bar{M}, \bar{R}_1, \bar{I})$ or $E_3^{(i)}(\bar{S}, \bar{M}, \bar{R}_2, \bar{I})$ for $i = 1, 2, 3$. Consequently, when the discriminant of Eq. (26) denoted by

$$\Delta_{f_3} = 18\vartheta_1\vartheta_2\vartheta_3 - 27\vartheta_3^2 + \vartheta_1^2\vartheta_2^2 - 4\vartheta_2^3 - 4\vartheta_1^3\vartheta_3,$$

is taken into consideration, Eq. (26) has one positive root if

$$\Delta_{f_3} \leq 0, \tag{29}$$

and three positive roots if

$$\Delta_{f_3} > 0. \tag{30}$$

iv. When \bar{M} is evaluated for equation (21)-(d), the equation $\Psi_1(\bar{M}) = \Psi_2(\bar{M})$ is reached such that $\Psi = \Psi_1(\bar{M}) = (1 - e^{-bM}) \frac{\gamma\bar{S}}{(\eta\bar{I}+\mu\bar{R}+v_M)}$ and $\Psi = \Psi_2(\bar{M}) = (\frac{\theta_M}{(\eta\bar{I}+\mu\bar{R}+v_M)} - \bar{M})$. In this case, the existence of a positive \bar{M} value can be proven using the graphical method in the $\bar{M} - \Psi$ coordinate plane. The graph showing the positive \bar{M} value is shown in Figure 2. Therefore, there is a positive equilibrium point $E_4^{(1)}(\bar{S}, \bar{M}, \bar{R}_1, \bar{I})$ or $E_4^{(1)}(\bar{S}, \bar{M}, \bar{R}_2, \bar{I})$.

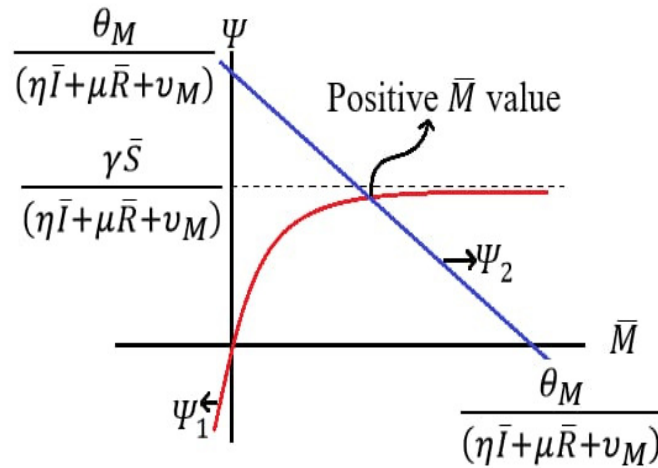


Figure 2. Graphical representation of the existence of a positive \bar{M} value for Eq. (21)-(d)

Local stability analysis

In this section, the LAS equilibrium points of the system (8) for each function shown in Table 4 have been examined. For this, the Jacobian matrix is calculated as

$$J = \begin{pmatrix} \gamma f_i(M) - v_S & (\eta I + \mu R + \gamma S \frac{df_i(M)}{dM}) & \mu M & \varepsilon \\ -\gamma f_i(M) & (-\eta I - \mu R - \gamma S \frac{df_i(M)}{dM} - v_M) & -\mu M & -\eta M \\ 0 & 0 & (r_R - 2R \frac{r_R}{C_R} + \sigma I - \beta) & \sigma R \\ 0 & 0 & 0 & -\omega \end{pmatrix}.$$

The equation of the eigenvalues for any the equilibrium point $(\bar{S}, \bar{M}, \bar{R}, \bar{I})$ from this matrix is

$$(\lambda^2 + (-\gamma f_i(\bar{M}) - v_S + v_M + \eta \bar{I} + \mu \bar{R} + \gamma \bar{S} \frac{df_i(M)}{dM} |_{M=\bar{M}}) \lambda + v_S (\eta \bar{I} + \mu \bar{R} + \gamma \bar{S} \frac{df_i(M)}{dM} |_{M=\bar{M}} + v_M - \frac{v_M}{v_S} \gamma f_i(\bar{M}))) (\lambda - (r_R - 2\bar{R} \frac{r_R}{C_R} + \sigma \bar{I} - \beta)) (\lambda + \omega) = 0. \tag{31}$$

From the second and third factor of Eq. (31), it is clear that $\lambda_3 = -\bar{R} \frac{r_R}{C_R} \in \mathbb{R}^-$ by (19)-(c) and $\lambda_4 = -\omega \in \mathbb{R}^-$ due to Ineq. (9). In this case, the eigenvalues λ_3 and λ_4 satisfies Ineq. (5).

Lastly, when the first factor of Eq. (31), in which the eigenvalues λ_1 and λ_2 are obtained, is taken into consideration, the characteristic equation is

$$\lambda^2 + \varkappa_1 \lambda + \varkappa_2 = 0, \tag{32}$$

where

$$\left\{ \begin{array}{l} \varkappa_1 = (-\gamma f_i(\bar{M}) - v_S + v_M + \eta \bar{I} + \mu \bar{R} + \gamma \bar{S} \frac{df_i(M)}{dM} |_{M=\bar{M}}) \\ \varkappa_2 = v_S (\eta \bar{I} + \mu \bar{R} + \gamma \bar{S} \frac{df_i(M)}{dM} |_{M=\bar{M}} + v_M - \frac{v_M}{v_S} \gamma f_i(\bar{M})) \end{array} \right\} \text{ for } i = 1, 2, 3, 4. \tag{33}$$

Thus, if the coefficients of Eq. (32) satisfy Ineqs. (5) and (6), the eigenvalues λ_1 and λ_2 satisfy the stability conditions for equilibrium point. Therefore, we have

$$\varkappa_1, \varkappa_2 > 0, \tag{34}$$

or:

$$\varkappa_1 < 0, 4\varkappa_2 > \varkappa_1^2, |\tan^{-1}(\frac{\sqrt{4\varkappa_2 - \varkappa_1^2}}{\varkappa_1})| > \frac{\phi\pi}{2}. \tag{35}$$

As a result, Table 5 regarding the equilibrium points can be accessed.

Table 5. Stability of equilibrium points obtained according to each functional response (for $i = 1, 2, 3$)

Response Type	Point	Existence Condition	LAS Condition
Holling Type 1	$E_1^{(1)}(\bar{S}, \bar{M}, \bar{R}_1, \bar{I})$	$\frac{v_M \bar{M} - (\theta_S + \theta_M)}{\varepsilon} < \bar{I}$	If $\bar{I} < \frac{\beta - r_R}{\sigma}$ and *
Holling Type 1	$E_1^{(1)}(\bar{S}, \bar{M}, \bar{R}_2, \bar{I})$	$\max\{\frac{\beta - r_R}{\sigma}, \frac{v_M \bar{M} - (\theta_S + \theta_M)}{\varepsilon}\} < \bar{I}$	If *
Holling Type 2	$E_2^{(1)}(\bar{S}, \bar{M}, \bar{R}_1, \bar{I})$	$\frac{v_M \bar{M} - (\theta_S + \theta_M)}{\varepsilon} < \bar{I}$	If $\bar{I} < \frac{\beta - r_R}{\sigma}$ and *
Holling Type 2	$E_2^{(1)}(\bar{S}, \bar{M}, \bar{R}_2, \bar{I})$	$\max\{\frac{\beta - r_R}{\sigma}, \frac{v_M \bar{M} - (\theta_S + \theta_M)}{\varepsilon}\} < \bar{I}$	If *
Holling Type 3	$E_3^{(1)}(\bar{S}, \bar{M}, \bar{R}_1, \bar{I})$	$\frac{v_M \bar{M} - (\theta_S + \theta_M)}{\varepsilon} < \bar{I}$	$\bar{I} \geq \frac{v_M \bar{M} + \frac{\theta_M}{\gamma} v_S - (\theta_S + \theta_M)}{\varepsilon}$ If $\bar{I} < \frac{\beta - r_R}{\sigma}$ and *
Holling Type 3	$E_3^{(1)}(\bar{S}, \bar{M}, \bar{R}_2, \bar{I})$	$\max\{\frac{\beta - r_R}{\sigma}, \frac{v_M \bar{M} - (\theta_S + \theta_M)}{\varepsilon}\} < \bar{I}$	If *
Holling Type 3	$E_3^{(i)}(\bar{S}, \bar{M}, \bar{R}_1, \bar{I})$	$\frac{v_M \bar{M} - (\theta_S + \theta_M)}{\varepsilon} < \bar{I}$	$\bar{I} < \frac{v_M \bar{M} + \frac{\theta_M}{\gamma} v_S - (\theta_S + \theta_M)}{\varepsilon}$ and $\Delta_{f_3} > 0$ If $\bar{I} < \frac{\beta - r_R}{\sigma}$ and *
Holling Type 3	$E_3^{(i)}(\bar{S}, \bar{M}, \bar{R}_2, \bar{I})$	$\max\{\frac{\beta - r_R}{\sigma}, \frac{v_M \bar{M} - (\theta_S + \theta_M)}{\varepsilon}\} < \bar{I}$	If *
Ivlev Type	$E_4^{(1)}(\bar{S}, \bar{M}, \bar{R}_1, \bar{I})$	$\frac{v_M \bar{M} - (\theta_S + \theta_M)}{\varepsilon} < \bar{I}$	If $\bar{I} < \frac{\beta - r_R}{\sigma}$ and *
Ivlev Type	$E_4^{(1)}(\bar{S}, \bar{M}, \bar{R}_2, \bar{I})$	$\max\{\frac{\beta - r_R}{\sigma}, \frac{v_M \bar{M} - (\theta_S + \theta_M)}{\varepsilon}\} < \bar{I}$	If *

*: Ineqs. (34) or (35) are satisfied

4 Estimation of derivative-order and parameters of the proposed model

The situation after the two major earthquakes with magnitudes (Kandilli Observatory) of Mw=7.7 in Kahramanmaraş, Pazarcık and Mw=7.6 in Kahramanmaraş, Elbistan, that occurred on 06.02.2023 was discussed in numerical studies. Therefore, the model in (8) was applied according to the parameters and derivative order determined for the Elbistan district. For this purpose, the following were done in order.

- In parameter estimations, time-dependent values of variables used in the system in (8) are needed. For this reason, in parameter estimation, data from the 1999 Gölcük earthquake in Türkiye were used in terms of its historical proximity, intensity, affected area, and results. The data set was determined accordingly.
- The model proposed in (8) was expressed through the ODE, and the parameters for each functional response were estimated with respect to real values by using the lsqcurvefit function of the Matlab R2024b software. In this way, the model parameters were found by determining the functional response that gave the minimum RMSE.
- Then, the derivative-order of the model with determined parameters was reduced by a precision of 0.01 and the most appropriate derivative-order was determined. The model with the parameters and derivative order that gave the minimum RMSE was determined as the best model.
- Finally, the results of the scenario with the relevant initial conditions for Elbistan after the Kahramanmaraş Elbistan earthquakes were presented.

Dataset

Türkiye is located in an earthquake zone and has witnessed many devastating earthquakes in history. In this sense, the largest earthquakes that have occurred here since the Republic period (1923-) are shown in [Table 6](#). The Kocaeli/Gölcük and Kahramanmaraş/Elbistan earthquakes

Table 6. Three major earthquakes experienced in Türkiye [39]

Date	Location	Magnitude	Deaths	Damaged Building
26.12.1939	Erzincan	7.9	32962	116720
17.08.1999	Kocaeli (Gölcük)	7.4	17479	43953
06.02.2023	Kahramanmaraş(Pazarcık-Elbistan)	7.7 and 7.6	50783	227027

are similar to each other in terms of the intensity of the earthquake, the number of deaths, the size of the affected area, and the closeness of their dates. In addition, the Gölcük earthquake was accepted as a reference for the Elbistan earthquake in terms of the accessibility of the variables (S , M , R and I in (8)) used in this study.

For parameter estimation, data following a 7.4 magnitude earthquake that hit the Kocaeli province of Türkiye on August 17, 1999, and whose epicenter was Gölcük, were used. Approximately 17479 people died in this earthquake and caused an estimated US\$6.5 billion in damage. The values used for parameter estimation are given in [Table 7](#).

The explanation of the variables in [Table 7](#) is as follows:

- P_1 : Total population for Kocaeli/Türkiye,
- P_2 : Migration population due to disaster for Kocaeli/Türkiye,
- Ratio: Population ratio (Gölcük Population/Kocaeli Population),
- $S(t)$: Total population for Gölcük district,
- $M(t)$: Migration population due to disaster according to population ratio for Gölcük district,
- $R(t)$: Number of flats according to building occupancy permit (for Residence Purposes) for Gölcük district,
- $I(t)$: SEDI for Gölcük district,
- $\frac{x}{\|x\|}$ for $x = t, S, M, R, I$: Vector normalization Values for Gölcük district.

Consider [Table 7](#). It is clear that $\|t\| = 9854.35559$, $\|S(t)\| = 710389.87055$, $\|M(t)\| = 8349.39620$, $\|R(t)\| = 118274.57312$ and $\|I(t)\| = 5.93951$. Data colored green are accepted as hypotheses. Data colored blue are data added according to the trend of the column data. Data colored in red were obtained according to population ratio (Gölcük/Kocaeli). In addition, the data colored yellow are the data augmented with ARIMA. Time data provides information for forecasting models. For this reason, the evaluation of these values in the model is useful for prediction. For forecasting using time data, along with classic ARIMA models, Prophet or LSTM models can be used with powerful recurrent neural network models [40, 41]. In this study, the ARIMA model was used to estimate the missing data.

ARIMA has a structure that uses a linear regression model to make forecasts on time series data in order to examine time-varying situations in patterns. The model automatically has regressive and moving average components, and its basic equation is as shown below.

$$Y_t = \partial_1 Y_{t-1} + \partial_1 Y_{t-2} + \dots + \partial_1 Y_{t-p} + \gamma_1 - \theta_1 \gamma_{t-1} - \gamma_2 - \theta_2 \gamma_{t-2} - \dots - \gamma_q - \theta_q \gamma_{t-q}, \quad (36)$$

∂_p , the parameter of the AR model, γ_q , error term coefficient, θ_q , the parameter value of the MA model and Y_t , shows the degree to which the data differs from the original data. In order to

Table 7. Time-dependent values of S, M, R and I variables after the Gölcük earthquake on 17 August 1999

t (Year)	P_1	P_2	S(t)	Ratio	M(t)	R(t)	I(t)	$\frac{t}{ t }$	$\frac{S(t)}{\ S(t)\ }$	$\frac{M(t)}{\ M(t)\ }$	$\frac{R(t)}{\ R(t)\ }$	$\frac{I(t)}{\ I(t)\ }$
1996	-	-	-	-	-	-	1.725715 [42]	-	-	-	-	-
2000	1206085 [43]	25000 [44]	107341 [44]	0.08900	2224.98829	1514	1.584858	0.202956	0.151102	0.266485	0.012801	0.266833
2001	1226460 [45]	24500	110862.6	0.09039	2214.61254	3099	1.549643	0.203057	0.156059	0.265242	0.026202	0.260904
2002	1259932 [45]	23510	114384.1	0.09079	2134.37724	4760	1.514429	0.203159	0.161016	0.255633	0.040245	0.254975
2003	1293594 [45]	22550	117905.7	0.09115	2055.33849	6373	1.479214	0.20326	0.165973	0.246166	0.053883	0.249046
2004	1328481 [45]	22250	121427.3	0.09140	2033.71928	7930	1.444 [42]	0.203362	0.170931	0.243577	0.067047	0.243118
2005	1364317 [45]	21400	124948.9	0.09158	1959.88649	9409	1.408154	0.203463	0.175888	0.234734	0.079552	0.237083
2006	1401013 [45]	20500	128470.4	0.09170	1879.81353	11009	1.372308	0.203565	0.180845	0.225144	0.09308	0.231047
2007	1437926 [46]	20000	131992 [46]	0.09179	1835.86638	12782	1.336462	0.203666	0.185802	0.21988	0.108071	0.225012
2008	1490358 [46]	19500	136513 [46]	0.09160	1786.15037	14791	1.300616	0.203768	0.192166	0.213926	0.125056	0.218977
2009	1522408 [46]	19300	136035 [46]	0.08936	1724.55446	16728	1.26477	0.203869	0.191493	0.206548	0.141434	0.212942
2010	1560138 [46]	18900	137637 [46]	0.08822	1667.37769	18450 [46]	1.228924	0.203971	0.193749	0.1997	0.155993	0.206907
2011	1601720 [46]	18000	141926 [46]	0.08861	1594.95293	19797 [46]	1.193078	0.204072	0.199786	0.191026	0.167382	0.200871
2012	1634691 [46]	17900	143867 [46]	0.08801	1575.35540	21231 [46]	1.157232	0.204174	0.202518	0.188679	0.179506	0.194836
2013	1676202 [46]	17750	145805 [46]	0.08699	1543.98978	23066 [46]	1.121386	0.204275	0.205246	0.184922	0.195021	0.188801
2014	1722795 [46]	17500	149238 [46]	0.08663	1515.94647	24816 [46]	1.08554	0.204377	0.210079	0.181564	0.209817	0.182766
2015	1780055 [46]	17480	152607 [46]	0.08573	1498.58873	26593 [46]	1.049694	0.204478	0.214821	0.179485	0.224841	0.176731
2016	1830772 [46]	17300	156901 [46]	0.08570	1482.64628	27807 [46]	1.013848	0.20458	0.220866	0.177575	0.235105	0.170696
2017	1883270 [46]	17100	161117 [46]	0.08555	1462.93452	29034 [46]	0.978002 [42]	0.204681	0.226801	0.175214	0.24548	0.16466
2018	1906391 [46]	16500	162584 [46]	0.08528	1407.18037	30635 [46]	0.960802	0.204783	0.228866	0.168537	0.259016	0.161765
2019	1953035 [46]	16000	165663 [46]	0.08482	1357.17383	33288 [46]	0.943602	0.204884	0.2332	0.162548	0.281447	0.158869
2020	1997258 [46]	15800	170503 [46]	0.08537	1348.82294	35738 [46]	0.926402	0.204985	0.240013	0.161547	0.302161	0.155973
2021	2033441 [46]	15750	172802 [46]	0.08498	1338.43642	38810 [46]	0.909202	0.205087	0.24325	0.160303	0.328135	0.153077
2022	2079072 [46]	15730	175940 [46]	0.08462	1331.14014	40897 [46]	0.892002 [42]	0.205188	0.247667	0.15943	0.34578	0.150181
2023	2102907 [46]	15700	177441 [46]	0.08438	1324.74888	42675.13044	0.874802	0.20529	0.24978	0.158664	0.360916	0.147285

make forecasting, the time-varying series must be stationary, and the simplest method for this is to observe the change based on the difference. The ARIMA equation (p, d, q) is obtained by performing a difference operation of degree d on the nonstationary ARMA model (p, q) . p is the degree of the AR model, d is the number of differences to make the data stationary, and q is the degree of the MA model.

Parameter estimation with minimum RMSE

The ODE form of (8) is

$$\begin{aligned}
 \frac{dS(t)}{dt} &= \theta_S + \eta MI + \mu MR + \gamma S f_i(M) + \varepsilon I - v_S S, \\
 \frac{dM(t)}{dt} &= \theta_M - \eta MI - \mu MR - \gamma S f_i(M) - v_M M, \\
 \frac{dR(t)}{dt} &= r_R R \left(1 - \frac{R}{C_R}\right) + \sigma RI - \beta R, \\
 \frac{dI(t)}{dt} &= \theta_I - \omega I, \\
 S(t_0) &= S_0, M(t_0) = M_0, R(t_0) = R_0, I(t_0) = I_0 \text{ such that } S_0, M_0, R_0, I_0 > 0.
 \end{aligned}
 \tag{37}$$

By using the data in the last five columns of Table 7, the parameter values obtained for each functional response of the (37) system are shown in Table 8. In addition, RMSE was used to

Table 8. Parameter values for each functional response of the Eqs. (37) and their RMSEs with respect to real values

Parameter	Holling Type-1	Holling Type-2	Holling Type-3	Ivlev Type
θ_S	41.75284	36.01879	31.54418	38.10101
η	112.49679	84.30196	170.74247	114.54013
μ	2.154	1.02587	0.1561	0.1561
γ	54.46518	1.9227	0.01217	0.01217
ε	0.0125891	15.27381	18.08166	0.0125891
v_S	30.7521	0.9157	1.02787	0.9157
θ_M	68.34056	1.2135	38.8599	44.87356
v_M	544.44999	240.7555	400.28472	441.69912
r_R	0.05191	2626.72693	2615.04485	0.05191
C_R	0.8752	0.32068	0.32034	0.08752
σ	29323.25997	642.82021	661.18863	22649.37148
β	4334.17795	3.5924	0.2324	2989.99665
θ_I	95.71375	0.2183	0.9715	17.13876
ω	733.45629	260.88913	266.48972	368.17729
b	Not available	36.13035	0.9965	0.24649
RMSE	0.100637153	0.121708496	0.120707238	0.116430262

compare the performances of functional responses with respect to real values. Accordingly, the function that gives the minimum RMSE compared to the others is the Holling Type-1 and the relevant graph can be seen in Figure 3.

Determining of the derivative-order to get lower RMSE

Here, the most appropriate derivative parameter has been investigated to take into account the delay in the model. The model giving the minimum RMSE was determined as for $i = 1$ (Holling Type-1). Now, the fractional model with first column parameters in Eq. (8) as regards Holling

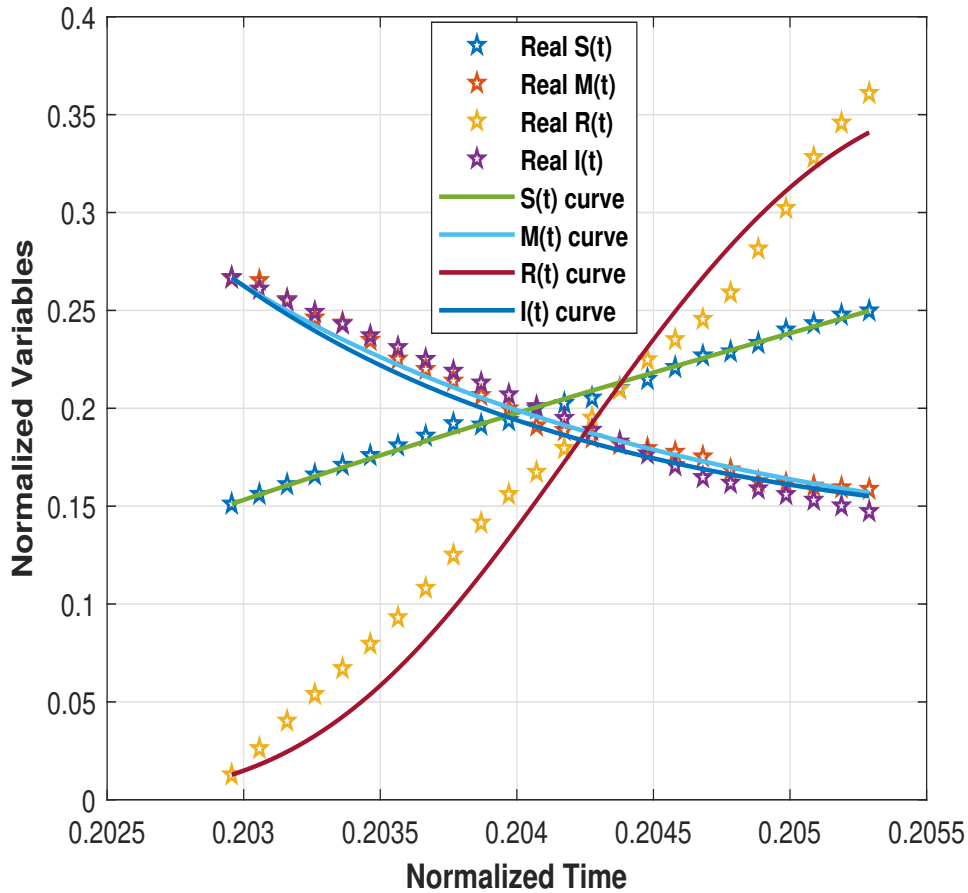


Figure 3. Graphical representation of the performance of system in (37) for Holling Type-1 functional response

Type-1 is as follows:

$$\begin{aligned}
 {}^{C}_{t_0}D_t^\phi S &= \theta_S + \eta MI + \mu MR + \gamma SM + \varepsilon I - v_S S, \\
 {}^{C}_{t_0}D_t^\phi M &= \theta_M - \eta MI - \mu MR - \gamma SM - v_M M, \\
 {}^{C}_{t_0}D_t^\phi R &= r_R R \left(1 - \frac{R}{C_R}\right) + \sigma RI - \beta R, \\
 {}^{C}_{t_0}D_t^\phi I &= \theta_I - \omega I,
 \end{aligned} \tag{38}$$

where $S(t_0) = S_0, R(t_0) = R_0, M(t_0) = M_0, I(t_0) = I_0$ such that $S_0, R_0, M_0, I_0 > 0$. In addition, the equilibrium points and their stabilities are calculated as follows. The equilibrium points are found as $E_1^{(1)}(1.72787, 0.10462, 0, 0.1305)$ and $E_1^{(2)}(1.72787, 0.67744, 0, 0.1305)$. Additionally, the coefficients of Eq. (32) are $\varkappa_1 = 616.7893, \varkappa_2 = 16986.19$ for $E_1^{(1)}$ and $\varkappa_1 = 33.23197, \varkappa_2 = -16986.2$ for $E_1^{(2)}$. Since these coefficients only for $E_1^{(1)}$ satisfy the equality in (34), the equilibrium point $E_1^{(1)}$ is LAS. The denormalized point corresponding to the LAS equilibrium point is $E_1^{(1)}(17027, 74319, 0, 0.775087)$.

By solving the system (38) with the Matlab R2023b software, the RMSE values corresponding to

different derivative orders are found as follows:

$$\begin{aligned}
 &0.143743817 \text{ for } \phi = 1.004, \\
 &0.124240729 \text{ for } \phi = 1.003, \\
 &0.110412390 \text{ for } \phi = 1.002, \\
 &0.103947676 \text{ for } \phi = 1.001, \\
 &0.105643008 \text{ for } \phi = 1.000, \\
 &0.114644800 \text{ for } \phi = 0.999, \\
 &0.129015936 \text{ for } \phi = 0.998, \\
 &0.146836443 \text{ for } \phi = 0.997, \\
 &0.166705461 \text{ for } \phi = 0.996.
 \end{aligned} \tag{39}$$

As can be clearly seen here, the derivative-order showing the best performance is determined as $\phi = 1.001$.

Numerical simulations of the model for Elbistan district after the earthquakes on 06.02.2023

The most recent earthquakes that caused major destruction in Türkiye are the following: Mw 7.7 (focal depth = 8.6 km) and Mw 7.6 (focal depth = 7km) with the epicenter in Pazarcık and Elbistan districts of Kahramanmaraş at 04:17 and 13:24 Türkiye time on February 6, 2023. These earthquakes are unprecedented disasters in recent history in terms of intensity and area covered. On the 51st day of the earthquakes, the death toll was announced as 50096. According to the report of the Ministry of Environment, Urbanization and Climate Change, it was determined that 224923 independent units in 50576 buildings, for which the damage assessment study was completed, were heavily damaged and collapsed, requiring urgent demolition. Especially severe consequences occurred in the Elbistan district of Kahramanmaraş, which was one of the epicenters of the earthquake. According to this report, 4943 houses were destroyed in Elbistan and the number of houses seriously damaged was 7238 [47]. In addition, the death toll from the earthquake was announced as 924.

For Elbistan, Figure 4 shows the time-dependent changes of the examined variables for three different derivative orders. The derivative order with minimum RMSE for model (38) has already been shown in (39). Here, graphs of the variables for Elbistan district are presented for three different values of ϕ : 0.901, 1.001 and 1.101. For $\phi = 1.001$, The model's 5-year forecast indicates: $S(t) \approx 150810$, $M(t) \approx 9473$, $R(t) \approx 620$ and $I(t) \approx 0.35$. Similarly, the model prediction for 10 years is the following: $S(t) \approx 173196$, $M(t) \approx 7131$, $R(t) \approx 166$ and $I(t) \approx 0.5$. According to the proposed model, it is estimated that Elbistan district will reach its pre-earthquake population size (141307) at the beginning of 2026.

According to Turkish Statistical Institute (TSI), the population data for Elbistan district decreased from 141307 for 2022 to 127755 ($S_0(t)$) for 2023 (after the earthquake) [46]. Therefore, it can be concluded that the number of population migrating after the earthquake in Elbistan district is approximately 12628 ($M_0(t)$). According to the statement of Elbistan Municipality, it was stated that most of the construction works of 4 thousand 12 houses ($R_0(t)$) created in the first stage have been completed. Considering the SEDI value of the Gölcük district between 1996 and 2000, there was an annual downward trend of 2.04%. SEDI-2022 for Elbistan was announced as 0.13 [42]. When the same trend is applied for Elbistan, the SEDI value will be 0.127348 for 2023 and 0.12475 for 2024.

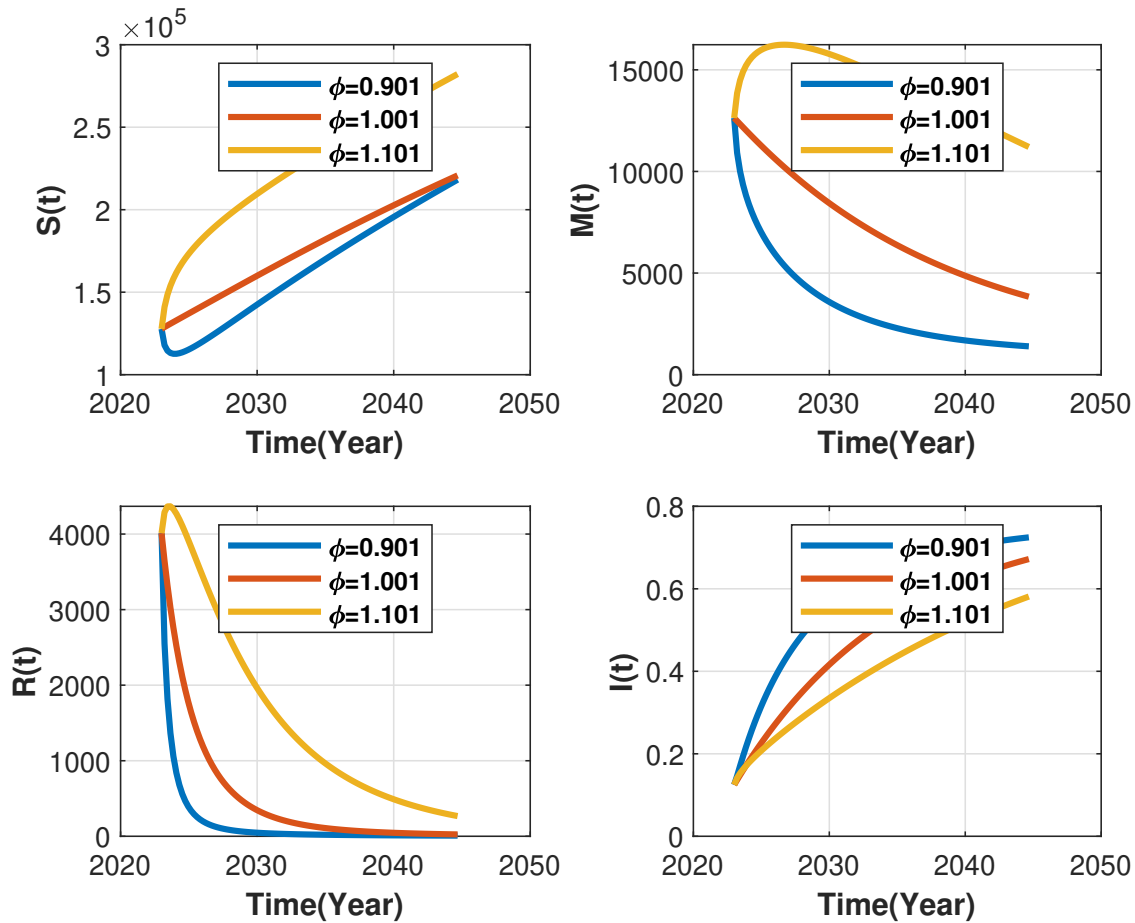


Figure 4. Time-dependent changes of S , M , R and I variables for Elbistan district

5 Conclusions

In the event of a disaster, different situations such as evacuation, leakage, containment, shelter, aid search, looting, theft, etc. may occur. Human nature tends to return to normal life after a disaster. For the surviving population post-disaster, there is a certain interaction between individuals who showed short-term panic behavior against such situations and migrated to a different region and individuals who continue to live in the disaster area within the means with controlled behavior. Thanks to this interaction, it is inevitable for the migrated population to exhibit controlled behavior and to have a tendency to return to the region when suitable conditions occur in the disaster area. In the model we proposed, we aimed to investigate the relationship between these two populations using different functional responses. Thus, it was aimed to find the functional response that gives the minimum RMSE by comparing the results of the proposed model with real data. Of course, the most important factors affecting the population after the disaster are whether the region has enough independent sections for settlement and socio-economic development of the region. Therefore, the effect of these variables on the population was also examined. The relationship between these variables is mathematically modeled using fractional order differential equations. In the model, there are four different functional responses. In numerical studies, parameter values were estimated using data from the 1999 Gölcük earthquake. Then, by changing the derivative order, the RMSE value was further reduced, and thus, the performance of the proposed model was increased. Lastly, the prediction results for Elbistan of FOS in (8) with Holling Type-1 functional response and derivative orders $\phi = 1.001$, is given in Table 9.

Table 9. The prediction results for Elbistan

<i>Time (Year)</i>	<i>S(t)</i>	<i>M(t)</i>	<i>R(t)</i>	<i>I(t)</i>	<i>Time (Year)</i>	<i>S(t)</i>	<i>M(t)</i>	<i>R(t)</i>	<i>I(t)</i>
2023	127755	12628	4012	0.12475	2034	177919	6712	131	0.520727
2024	132890	11877	2521	0.181987	2035	182580	6321	106	0.543116
2025	136879	11294	1782	0.224046	2036	186263	6027	90	0.559603
2026	141860	10606	1190	0.272454	2037	190807	5682	74	0.578579
2027	146836	9960	819	0.316618	2038	194395	5423	64	0.592552
2028	150808	9473	620	0.349146	2039	198820	5118	53	0.608633
2029	155749	8900	448	0.386588	2040	203178	4834	45	0.623302
2030	160656	8365	331	0.420747	2041	206618	4621	40	0.634103
2031	164551	7961	264	0.445904	2042	210859	4370	34	0.646533
2032	169376	7488	203	0.474859	2043	215037	4137	30	0.657871
2033	173196	7131	166	0.496184	2044	218334	3962	27	0.666219

The purpose of population forecasts is to determine the size of workforce that will be needed in the future and to prepare the infrastructure and facilities accordingly. Population projections help identify future risks and opportunities, make plans, and take precautions. Thus, it is important to estimate the future population in a region after a disaster in the light of certain parameters, and mathematical methods are used for this. Public institutions and organizations aim to achieve their social and economic target plans within the stipulated time in order for a region to reach its pre-disaster population structure. Thanks to the results of the model we propose, predictions are made about whether they will achieve these goals in the specified time period. It adds innovation to the literature in terms of the structure of the mathematical model used, its analysis, and adaptation of the results to the real world example.

The model and analysis proposed in this study are extremely useful in terms of their applicability to natural disasters such as tsunamis and landslides occurring in different parts of the world.

Declarations

Use of AI tools

The authors declare that they have not used Artificial Intelligence (AI) tools in the creation of this article.

Data availability statement

No Data associated with the manuscript.

Ethical approval (optional)

The authors state that this research complies with ethical standards. This research does not involve either human participants or animals.

Consent for publication

Not applicable

Conflicts of interest

The authors declare that they have no conflict of interest.

Funding

This study was supported by Scientific and Technological Research Council of Türkiye (TUBITAK) under the Grant Number 123F220 (TUBITAK 1002).

Author's contributions

T.D.: Writing - Original Draft Preparation – Review & Editing, Validation. B.D.: Conceptualization, Methodology, Data Curation, Writing-Original Draft Preparation, Formal Analysis, Validation, Software. All authors have read and agreed to the published version of the manuscript.

Acknowledgements

The authors thank to TUBITAK for their support.

References

- [1] Chaudhary, M.T. and Piracha, A. Natural disasters-origins, impacts, management. *Encyclopedia*, 1(4), 1101-1131, (2021). [[CrossRef](#)]
- [2] Asian Disaster Reduction Center. Natural disaster data book 2022 (an analytical overview). (2022). https://www.adrc.asia/publications/databook/ORG/databook_2022/pdf/DataBook2022.pdf
- [3] AFAD, Afet Türleri, (2023). <https://www.afad.gov.tr/afet-turleri>
- [4] Verdière, N., Lanza, V., Charrier, R., Provitolo, D., Dubos-Paillard, E., Bertelle, C. and Alaoui, A. Mathematical modeling of human behaviors during catastrophic events. In *Proceedings, 4th International Conference on Complex Systems and Applications (ICCSA)*, pp. 67-74, Le Havre, France, (2014, June).
- [5] Paul, B.K. Evidence against disaster-induced migration: the 2004 tornado in north-central Bangladesh. *Disasters*, 29(4), 370-385, (2005). [[CrossRef](#)]
- [6] Tuncer, G. Türkiye’de sosyo-ekonomik gelişmişliğin mekânsal eşitsizliği. *Journal of Economics Public Finance Business*, 2(2), 69-80, (2019).
- [7] Boğaziçi University, Kandilli Observatory and Earthquake Research Institute, Regional Earthquake-Tsunami Monitoring and Evaluation Center, (2024). <http://udim.koeri.boun.edu.tr/zeqmap/hgmmmap.asp>
- [8] Ozaslan, M., Dincer, B. and Ozgur, H. Regional disparities and territorial indicators in Turkey: Socio-economic development index (SEDI). In *Proceedings, 46th Congress of the European Regional Science Association: "Enlargement, Southern Europe and the Mediterranean"* (ERSA), pp. 1-34, Volos, Greece, (2006, August).
- [9] Du, M., Wang, Z. and Hu, H. Measuring memory with the order of fractional derivative. *Scientific Report*, 3, 3431, (2013). [[CrossRef](#)]
- [10] Avci, D., Ozdemir, N. and Yavuz, M. Fractional optimal control of diffusive transport acting on a spherical region. In *Methods of Mathematical Modelling* (pp. 63-82). Boca Raton, USA: CRC Press, (2019).
- [11] Paul, S., Mahata, A., Mukherjee, S., Mali, P. and Roy, B. Fractional order SEIQRD epidemic model of COVID-19: A case study of Italy. *PLoS One*, 18(3), e0278880, (2023). [[CrossRef](#)]
- [12] Husnain, S. and Abdulkader, R. Fractional order modeling and control of an articulated robotic arm. *Engineering, Technology & Applied Science Research*, 13(6), 12026-12032, (2023). [[CrossRef](#)]

- [13] Joshi, H. and Yavuz, M. Transition dynamics between a novel coinfection model of fractional-order for COVID-19 and tuberculosis via a treatment mechanism. *The European Physical Journal Plus*, 138(5), 468, (2023). [[CrossRef](#)]
- [14] Ersoy, B., Daşbaşı, B. and Aslan, E. Mathematical modelling of fiber optic cable with an electro-optical cladding by incommensurate fractional-order differential equations. *An International Journal of Optimization and Control: Theories & Applications (IJOCTA)*, 14(1), 50-61, (2024). [[CrossRef](#)]
- [15] Kumar, D., Nama, H. and Baleanu, D. Dynamical and computational analysis of fractional order mathematical model for oscillatory chemical reaction in closed vessels. *Chaos, Solitons & Fractal*, 180, 114560, (2024). [[CrossRef](#)]
- [16] Moya, E.M.D., Rodriguez, R.A., Pietrus, A. and Bernard, S. A study of fractional optimal control of overweight and obesity in a community and its impact on the diagnosis of diabetes. *Mathematical Modelling and Numerical Simulation with Applications*, 4(4), 514-543, (2024). [[CrossRef](#)]
- [17] Iwa, L.L., Omame, A. and Inyama, S.C. A fractional-order model of COVID-19 and Malaria co-infection. *Bulletin of Biomathematics*, 2(2), 133-161, (2024). [[CrossRef](#)]
- [18] Adu, I.K., Wireko, F.A., Adarkwa, S.A. and Agyekum, G. O. Mathematical analysis of Ebola considering transmission at treatment centres and survivor relapse using fractal-fractional Caputo derivatives in Uganda. *Mathematical Modelling and Numerical Simulation with Applications*, 4(3), 296-334, (2024). [[CrossRef](#)]
- [19] Daşbaşı, B. Fractional order bacterial infection model with effects of anti-virulence drug and antibiotic. *Chaos, Solitons & Fractals*, 170, 113331, (2023). [[CrossRef](#)]
- [20] Helbing, D., Farkas, I. and Vicsek, T. Simulating dynamical features of escape panic. *Nature*, 407, 487-490, (2000). [[CrossRef](#)]
- [21] Provitolo, D. A new classification of catastrophes based on “Complexity Criteria”. In *From System Complexity to Emergent Properties* (pp. 179-194). Berlin, Heidelberg: Springer, (2009). [[CrossRef](#)]
- [22] Yang, J., Yokoo, M., Ito, T., Jin, Z. and Scerri, P. *Principles of Practice in Multi-Agent Systems*. Springer: Berlin, (2009).
- [23] Kumar, S., Singh, R., Singh, B.K. and Garg, R. Mathematical model for estimating flood disaster effect on a population by using differential equation. *International Journal of Computational Modeling and Physical Sciences*, 1(2), 14-18, (2021).
- [24] Verdière, N., Cantin, G., Provitolo, D., Lanza, V., Dubos-Paillard, E., Charrier, R. et al. Understanding and simulation of human behaviors in areas affected by disasters: From the observation to the conception of a mathematical model. *Global Journal of Human Social Science: H Interdisciplinary*, 15(10-H), (2015).
- [25] Hassell, M.P. *The Dynamics of Arthropod Predator-Prey Systems*. Princeton University Press: New Jersey, (1978).
- [26] Xu, H. and Zou, S. A diffusive Monod-Haldane predator-prey system with Smith growth and a protection zone. *Nonlinear Analysis: Real World Applications*, 76, 104018, (2024). [[CrossRef](#)]
- [27] Allen, L.J.S. *An Introduction to Mathematical Biology*. Pearson Prentice Hall: Italy, (2007).
- [28] Holling, C.S. Some characteristics of simple types of predation and parasitism. *The Canadian Entomologist*, 91(7), 385-398, (1959). [[CrossRef](#)]

- [29] Kooij, R.E. and Zegeling, A. A predator-prey model with Ivlev's functional response. *Journal of Mathematical Analysis and Applications*, 198(2), 473-489, (1996). [[CrossRef](#)]
- [30] Uddin, M.J., Santra, P.K., Rana, S.M.S. and Mahapatra, G. Chaotic dynamics of the fractional order predator-prey model incorporating Gompertz growth on prey with Ivlev functional response. *Chaos Theory and Applications*, 6(3), 192-204, (2024). [[CrossRef](#)]
- [31] Caputo, M. and Fabrizio, M. A new definition of fractional derivative without singular kernel. *Progress in Fractional Differentiation & Applications*, 1(2), 73-85, (2015). [[CrossRef](#)]
- [32] Odibat, Z.M. and Shawagfeh, N.T. Generalized Taylor's formula. *Applied Mathematics and Computation*, 186(1), 286-293, (2007). [[CrossRef](#)]
- [33] Matignon, D. Stability results for fractional differential equations with applications to control processing. In Proceedings, *Computational Engineering in Systems Applications*, pp. 963-968, Paris, France, (1996, July).
- [34] Rostamy, D. and Mottaghi, E. Stability analysis of a fractional-order epidemics model with multiple equilibriums. *Advances in Difference Equations*, 2016, 170, (2016). [[CrossRef](#)]
- [35] Daşbaşı, B. The Fractional-Order mathematical modeling of bacterial resistance against multiple antibiotics in case of local bacterial infection. *Sakarya University Journal of Science*, 21(3), 442-453, (2017). [[CrossRef](#)]
- [36] Wang, X. A simple proof of Descartes's rule of signs. *The American Mathematical Monthly*, 111(6), 525-526, (2004). [[CrossRef](#)]
- [37] Li, Y., Chen, Y. and Podlubny, I. Stability of fractional-order nonlinear dynamic systems: Lyapunov direct method and generalized Mittag-Leffler stability. *Computers & Mathematics with Applications*, 59(5), 1810-1821, (2010). [[CrossRef](#)]
- [38] Li, H.L., Zhang, L., Hu, C., Jiang, Y.L. and Teng, Z. Dynamical analysis of a fractional-order predator-prey model incorporating a prey refuge. *Journal of Applied Mathematics and Computing*, 54, 435-449, (2017). [[CrossRef](#)]
- [39] Peker, A.E. and Şanlı, İ. Deprem ve göç ilişkisi: 24 Ocak 2020 Elazığ deprem örneği. *Firat University International Journal of Economics and Administrative Sciences*, 6(1), 125-154, (2022).
- [40] Box, G.E. and Jenkins, G.M. Time series analysis, control, and forecasting. *San Francisco, CA: Holden Day*, 3226(3228), 10, (1976).
- [41] Arslan, R.S., Barışçı, N., Arici, N. and Kocer, S. Detecting and correcting automatic speech recognition errors with a new model. *Turkish Journal of Electrical Engineering and Computer Sciences*, 29(5), 2298-2311, (2021). [[CrossRef](#)]
- [42] Republic of Türkiye Ministry of Industry and Trade, Socio-Economic Development Ranking Research Reports, (2024). <https://www.sanayi.gov.tr/merkez-birimi/b94224510b7b/sege/ilce-sege-raporlari>
- [43] Turkish Statistical Institute, 2000 General Population Census, (2000). <https://biruni.tuik.gov.tr/nufusapp/idari.zul>
- [44] Sudaş, İ. 17 Ağustos 1999 Marmara depreminin nüfus ve yerleşme üzerindeki etkileri: Gölcük (Kocaeli) örneği. *Aegean Geographical Journal*, 13, 73-91, (2004).
- [45] Wikipedia, Kocaeli/ (province), (2023). [https://fr.wikipedia.org/wiki/Kocaeli_\(province\)](https://fr.wikipedia.org/wiki/Kocaeli_(province))
- [46] Turkish Statistical Institute, Address-Based Population Registration System Results, (2024). <https://biruni.tuik.gov.tr/medas/?locale=tr>

- [47] Presidency of the Republic of Turkey, Strategy and Budget Directorate, 2023 Kahramanmaraş and Hatay Earthquakes Report, (2023). <https://www.sbb.gov.tr/wp-content/uploads/2023/03/2023-Kahramanmaras-ve-Hatay-Depremleri-Raporu.pdf>

Mathematical Modelling and Numerical Simulation with Applications (MMNSA)
(<https://dergipark.org.tr/en/pub/mmnsa>)



Copyright: © 2025 by the authors. This work is licensed under a Creative Commons Attribution 4.0 (CC BY) International License. The authors retain ownership of the copyright for their article, but they allow anyone to download, reuse, reprint, modify, distribute, and/or copy articles in MMNSA, so long as the original authors and source are credited. To see the complete license contents, please visit (<http://creativecommons.org/licenses/by/4.0/>).

How to cite this article: Daşbaşı, T. & Daşbaşı, B. (2025). Fractional-order model of the post-disaster period: study on the earthquakes in Türkiye. *Mathematical Modelling and Numerical Simulation with Applications*, 5(1), 117-142. <https://doi.org/10.53391/mmnsa.1503311>